Optics Communications 285 (2012) 2729–2733

Contents lists available at SciVerse ScienceDirect

Optics Communications

journal homepage: www.elsevier.com/locate/optcom

Z-scan study of nonlinear absorption of gold nano-particles prepared by ion implantation in various types of silicate glasses

W. Husinsky [a], A. Ajami [a,*], P. Nekvindova [b], B. Svecova [b], J. Pesicka [c], M. Janecek [c]

[a] Institute of Applied Physics, Vienna University of Technology, Wiedner Huaptstrasse 8-10 Wien-1040, Austria
[b] Department of Inorganic Chemistry, Faculty of Chemical Technology, Institute of Chemical Technology, Technicka 5, 166 28 Prague, Czech Republic
[c] Charles University, Faculty of Mathematics and Physics, Department of Physics of Materials, Ke Karlovu 5, 121 16 Prague, Czech Republic

ARTICLE INFO

Article history:
Received 21 March 2011
Received in revised form 19 December 2011
Accepted 25 January 2012
Available online 9 February 2012

Keywords:
Silicate glass
Metal nano-particles
Nonlinear absorption
Au+ ion implantation
Z-scan
Ultra short lasers

ABSTRACT

Metal nano-clusters composite glasses synthesized by ion implantation have been shown as promising nonlinear photonic material. In this paper, we report on the nonlinear absorption measurements of gold nano-particles implanted in four structurally different types of silicate glasses. All targets containing gold nano-particles in a layer 500 nm under the surface of the glass have been prepared by ion implantation with subsequent annealing. The targets were characterized by UV–VIS absorption spectroscopy, transmission electron microscopy (TEM) and by the Z-scan technique. The resulting nano-particles differed in size, range of particle size and shape as well as depth distribution characteristic for glasses with different chemical compositions. With the Z-scan technique, it can be shown that the nano-particles produced in silicate glasses exhibit substantial two-photon absorption (TPA). The TPA coefficient differed depending on size, shape, and depth distribution of the metal nano-clusters and the structure and composition of the glass substrates. The highest TPA coefficient (16.25 cm/GW) was found for the glass BK7 in which the largest non-spherical nano-particles have been observed in the thinnest layer.

1. Introduction

Glass substrates have recently attracted growing interest due to the fact that they can serve as substrates for nano-structured systems with remarkable optical nonlinear properties [1]. Glass substrates possess overall advantages as compared to many crystals or polymers. In particular, the composition of the glass can be well designed and tuned according to the needs of the encompassed photonic components and also their fabrication is usually feasible and inexpensive [2]. Silicate glasses (i.e., glasses based on silica SiO_2) are both chemically and thermally stable, and it is rather simple to fabricate waveguides compatible with currently used optical fibers.

The metal nano-cluster composite glasses synthesized by ion implantation have been shown as particularly promising nonlinear photonic materials [1,3–6]. Nanometric metal particles can exhibit a nonlinear optical response several orders of magnitude larger than bulk metals due to a phenomenon referred to as surface plasmon resonance. When the particle size ranges from nanometer to a few tens of nanometers, confinement results in the possibility of resonantly exciting the electron gas collectively by coupling with an appropriate oscillating electromagnetic field. As the local electric field in the particles is enhanced due to the oscillation of the electron gas, the metal nonlinear optical response can be amplified as compared to the bulk solid one [7].

Recent experiments have shown that standard glass substrates containing nano-particles of Au can be regarded as one of the most promising nonlinear optical materials [8–16]. The experiments have shown that such materials exhibit very strong nonlinear third-order susceptibility. $\chi^{(3)}$ contains a real and an imaginary part. The real part of the susceptibility is related to the refractive index while the imaginary part determines the absorption coefficient. Therefore, a strong third-order nonlinear optical response might manifest itself as a noticeable change in the refractive index or in the absorption coefficient or in both.

The third-order nonlinear optical process is responsible for nonlinear behaviors such as the optical Kerr effect, two-photon absorption, third harmonic generation and many more. These phenomena can be observed in almost all materials when they are irradiated with high intense laser radiation such as ultrashort laser pulses. For the Kerr effect and two-photon absorption, the nonlinear optical response is observed as a linear intensity dependence in the refractive index and in the absorption coefficient respectively.

$$n(I) = n_0 + \gamma I \tag{1.a}$$

$$\alpha(I) = \alpha_0 + \beta I \tag{1.b}$$

where n_0 is the linear refractive index, γ is the nonlinear index of refraction, α_0 is the linear absorption coefficient, β is the two-photon

* Corresponding author.
E-mail address: ali_ajami80@yahoo.com (A. Ajami).

0030-4018/$ – see front matter © 2012 Elsevier B.V. All rights reserved.
doi:10.1016/j.optcom.2012.01.044

absorption coefficient and I denotes the irradiance of the laser beam within the nonlinear medium.

The ratio of the imaginary to the real parts of the third-order nonlinear susceptibility is given by $\beta/k\gamma$ (where k is the wave number) which determines the absorptive and refractive contributions to the third-order nonlinear susceptibility. Depending on this ratio, metal nano-cluster composite materials can be employed for different applications. For instance, in the case $\beta > k\gamma$, the absorptive property can be exploited for a variety of optical limiting applications (protective devices etc.) [17,18] whereas for $\beta < k\gamma$, the refractive properties can be exploited for all-optical switching devices [14,19].

Third-order nonlinear optical properties of metal/dielectric nanocomposite materials depend significantly on many factors regarding both the materials themselves (metal and host medium kinds, metal particles concentration, size and shape) and the excitation laser (wavelength, intensity, pulse width) [13,20–23].

Several different experimental methods can be employed to measure TPA coefficients such up-converted fluorescence emission [24], transient absorption [25], four-wave mixing [26] and the Z-scan technique [27,28]. Among these methods the Z-scan technique, which was first introduced by Sheik-Bahae et al. in 1989 [29], is a particularly sensitive technique. It is especially suitable for non-fluorescence materials such as metal nano-cluster composite materials for which the up-converted fluorescence emission experiment is not an appropriate method for measuring TPA coefficient. In this technique the nonlinear medium is translated along the laser beam propagation direction through the focal point of a tightly focused laser beam. The transmitted energy through the sample is entirely collected using a convergent lens and detected by a diode. The measured signal is a V-shape curve from which the nonlinear absorption coefficient can be extracted.

We had previously found significant differences of the ion penetration depth for various glass substrates when implanted with Au^+ ions [30]. In this paper we focused on the measurement of nonlinear absorption and the study of the relationship between the nonlinear absorption and the size, depth distribution and shape of gold nanoparticles and also the structure of silicate glasses. Four types of silicate glasses with different compositions (the variation was mainly due to different concentrations of monovalent modifiers and, therefore, in the extent of cross-linking of glass matrix) were chosen according to our previous study [31]. The glasses were implanted with Au^+ ions under identical conditions; the nucleation of metal nanoparticles was initiated during the subsequent annealing of the as-implanted glasses. In the case of post-implantation annealing, the conditions were also kept identical for all prepared samples. Formation and evolution of the metal nano-particles in the glass substrates were studied by absorption spectroscopy and TEM. Nonlinear absorption was measured by the open aperture Z-scan technique.

We have also addressed the question, if and in how far it is possible to influence and control the nonlinear properties of the resulting composite glass–metal material. The results were evaluated in terms of finding and understanding the relations between the properties of the composite glass–metal material and the properties of the implantation particles, which may be of crucial importance in designing e.g. nano-particles based components for special applications.

2. Experimental

2.1. Preparation of samples

We have used four types of optical silicate glasses, namely specially designed GIL49 and Glass B (made at the Glass Institute Hradec Kralove Ltd., Czech Republic) and commercially available silica glass and BK7. The used glasses varied especially in the concentration of monovalent modifiers (Na_2O, K_2O) as well as their network formers (SiO_2, B_2O_3). The compositions of the glasses can be found in Table 1.

The thoroughly pre-cleaned glass substrates were implanted with Au^+ ions at an energy of 1701 keV while the ion fluence was kept at 1×10^{16} ions cm^{-2}. The implantation was performed at the Tandetron 4130 MC accelerator at the Nuclear Physics Institute in Prague, Czech Republic. The as-implanted glasses were annealed in air at temperature of 600 °C for 5 h.

2.2. Characterization of sample properties

The depth distribution and diffusion profiles of the implanted Au were investigated using Rutherford Backscattering Spectrometry (RBS) with 2.0 MeV He^+ ions at the Nuclear Physics Institute in Prague, Czech Republic and have already been reported in Ref. [30]. UV–VIS absorption spectra were collected using a dual-beam spectrometer (CARY 50) in transmission modes ranging from 300 to 1000 nm at the Institute of Chemical Technology Prague, Czech Republic.

Nano-particle microscopy characterization was done by a TEM (JEOL 2000 FX) equipped with an energy dispersive X-ray analyzer (Link AN 10000) at the Faculty of Mathematics and Physics, Charles University Prague, Czech Republic. The samples were prepared with a dimple grinder (Gatan Inc.) and by ion polishing procedure with a precise ion polishing system (Gatan PIPS) for thin foil preparation for TEM.

Nonlinear absorption was measured applying the open aperture Z-scan technique for ultrashort laser radiation. A Ti:sapphire laser (FEMTOPOWER Compact PRO) was used that delivers ultra short laser pulses at a repetition rate of 1 kHz each pulse having a maximum energy of 1 mJ with a spectrum centered at 790 nm. The duration of the shortest pulses for this system, estimated as the full width at half maximum (FWHM) of a Gaussian temporal profile, is 25 fs. There is a possibility for pulses to be stretched up to a few hundreds of femto-second using a Dazzler system (an acousto-optic programmable dispersive filter). An autocorrelator (model: ENV40CSG, Femtolasers) was employed to measure the pulse duration. The laser beam power was measured using a digital power meter in front of the sample prior to each measurement. A 175 mm focal length plano-convex lens was used to focus the 15 mm diameter laser beam within the sample. The Rayleigh range and beam waist radius were measured to be 0.28 mm and 11 μm respectively considering this fact that the beam quality factor is 2 for our laser system. The sample mounted on a translating stage was moved 6 mm from 3 mm before the focus to 3 mm after the focus in about 40 steps. The schematic of the experimental setup is shown in Fig. 1 and has been described in detail elsewhere [32].

3. Results

3.1. Linear absorption spectra and characteristics of nano-clusters

The measurements of the optical absorption spectra indicated different spectra for as-implanted and as-annealed samples as shown in Fig. 2. It can be seen from Fig. 2 that no significant increase of the linear absorption in UV–VIS region occurred for any prepared sample after the ion implantation. After annealing, except for the silica glass, the targets attained a pink–red color, which was proven by the presence of an absorption peak in UV–VIS region. Although the

Table 1
The compositions of the silicate substrates (in wt.%).

Glass substrate	SiO_2	Na_2O	Al_2O_3	CaO	MgO	K_2O	B_2O_3	BaO
GIL49	63.2	24.4	1.1	5.6	5.3	0.5	–	–
Glass B	88.0	8.7	3.3	–	–	–	–	–
BK7	68.3	8.8	–	0.1	–	8.1	12.1	2.5
Silica glass	100	–	–	–	–	–	–	–

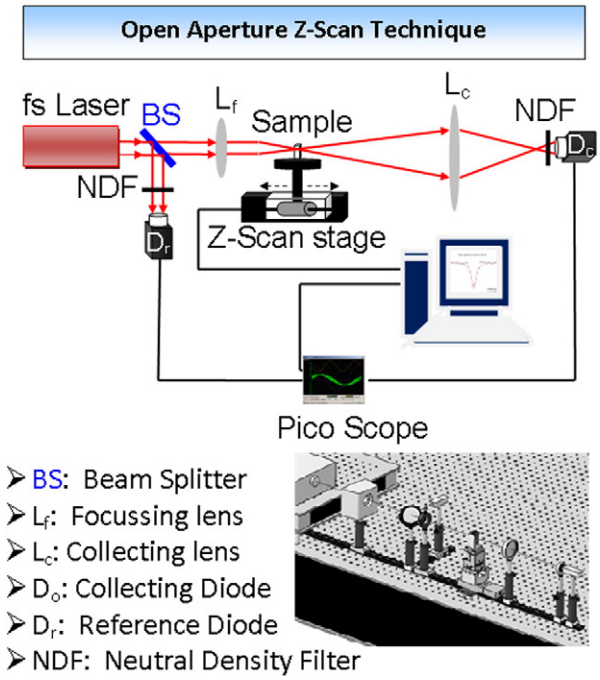

Fig. 1. Schematic of the Z-scan experimental setup.

experimental conditions were kept identical for the treatment of all samples but their absorption spectra showed different peaks after annealing. Two as-annealed samples GIL49 and BK7 each one showed one absorption peak at 525 nm and 560 nm respectively but as-annealed glass B showed two absorption peaks at 415 and 520 nm.

Glasses with absorption in the visible region after annealing were characterized by TEM and details of the results will be published separately. TEM analysis confirmed the presence of metal nano-particles in as-annealed glasses at a depth corresponding well to the depth of the maximum Au concentration measured by RBS. The most relevant results of the characterization of the nano-structures obtained by TEM analysis for all samples are summarized in Table 2.

From Table 2, it is evident that the size and shape of the gold nano-particles differ for the various types of glass although all the glasses were treated under identical conditions. Nano-particles observed in glass B were small (1–7 nm) and were present in a relatively broad layer of 350 nm. In glass GIL49, nano-particles with different sizes from 1 to 15 nm were found in a layer of 250 nm. Nano-particles in BK7 glass were typically 6–25 nm and were concentrated in a narrow layer of 100 nm.

3.2. Determinations of TPA coefficients

In the first step we have determined the laser parameter regime in which TPA can be clearly attributed (from the measured Z-scans) to the existence of gold nano-clusters. By varying the pulse duration from 25 fs to 200 fs (possible range of our laser system) we observed no dependence on the pulse duration. We decided to perform all the measurements with the shortest pulses possible (25 fs). Furthermore, it had to be verified that no nonlinear absorption is due to the glass substrates themselves. For this purpose, we first determined the intensity at which the standard glass (i.e. non implanted glass) starts exhibiting nonlinear absorption. The pulse energy threshold for nonlinear absorption of the standard glasses was determined to be 50 nJ. Therefore, all the Z-scan measurements for the as-implanted and as-annealed samples were performed with pulse energies lower than 50 nJ. In this intensity regime the Z-scan results depend on the laser pulse energy, i.e. the nonlinear absorption of the sample increases with increasing pulse energy (see Fig. 4).

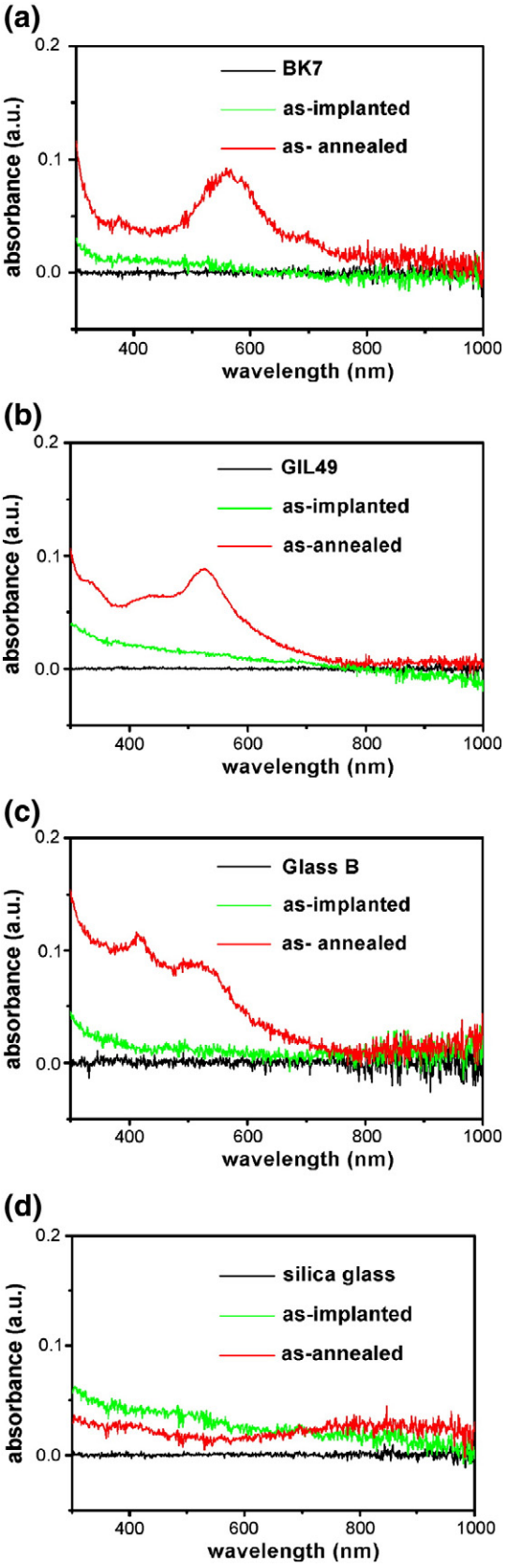

Fig. 2. UV–VIS absorption spectra of four different types of silicate glass substrates implanted and annealed under identical conditions. (a) BK7; (b) GIL49; (c) glass B; (d) silica glass.

Table 2
The TEM analysis of four different silicate glass substrates implanted and annealed under identical conditions.

Glass substrate	Thickness of layer with nano-particles	Size of nano-particles	Shape of nano-particles
Silica glass	Not measured	Not measured	Not measured
GIL49	250 nm	1–15 nm	Spherical
Glass B	350 nm	1–7 nm	Spherical
BK7	100 nm	6–25 nm	Non-spherical

In the next step, the as-implanted glasses were measured. It was found that only as-implanted glass BK7 showed nonlinear absorption. The TPA coefficient was determined by fitting Eq. (2) to the Z-scan experimental data.

$$T(z) = \sum_{n=0}^{\infty} \frac{(-q_0)^n}{(n+1)^{3/2}(1+x^2)^n} \tag{2}$$

where q_0 is $\beta L I_0$, β is the TPA coefficient, L is the thickness of the sample (gold nano-particles layer), $x = z/z_0$, z is the sample position, z_0 is the Rayleigh range and I_0 is the maximum on-axis intensity at the focal point of the laser beam within the sample. It should be noted that Eq. (2) is used to extract the pure TPA coefficient under assumption of negligible excited state absorption and three-photon or higher order nonlinear absorption as described in Ref. [32]. The obtained TPA coefficient for as-implanted BK7 is 11.08 cm/GW.

In the next step, the influence of annealing on the TPA of the resulting nano-composite material has been studied. Fig. 3 shows Z-scans of as-implanted and as-annealed BK7 performed with the same pulse energy of 30 nJ. It is evident from Fig. 3 that the TPA for BK7 showed a 40% increase after annealing. Fig. 4 shows Z-scans of as-annealed glass BK7 measured with different pulse energies. As can be seen from Fig. 4, the normalized absorbance increases linearly with laser pulse energy (laser intensity), which is an indication of TPA due to the presence of gold nano-particles in BK7. The same measurements were performed for all other as-annealed samples. The obtained TPA coefficients for all samples are summarized in Table 3 and also are compared in Fig. 5.

The highest TPA coefficient of 16.25 cm/GW was obtained for as-annealed BK7 that had developed the largest non-spherical nano-particles in the thinnest layer of 100 nm whereas the smallest TPA coefficient of 2.46 cm/GW was obtained for as-annealed silica glass that showed no absorption in the UV–VIS region. It should also be mentioned that the linear absorption at a wavelength of 790 nm was negligible for all samples. Hence no saturation of absorption at this wavelength for these samples can be expected.

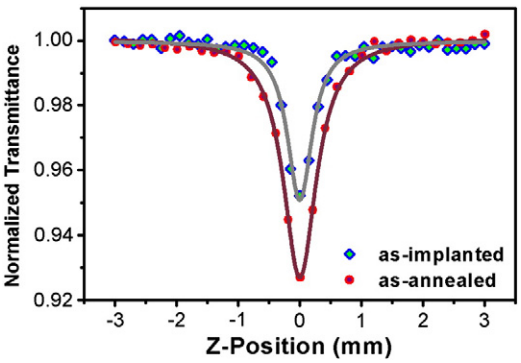

Fig. 3. Z-scans of the as-implanted and as-annealed glass BK7 measured with the same pulse energy of 30 nJ. Blue solid line represents the best fit to the experimental data for the as-implanted sample and red solid line is for the as-annealed sample.

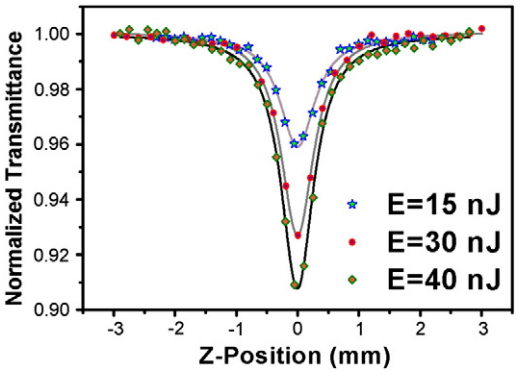

Fig. 4. Z-scans of as-annealed glass BK7 possessing a 100 nm thick layer of gold nano-particles after annealing performed with different pulse energies.

4. Discussion

A different nucleation of gold nano-particles observed in our glasses after the annealing process is probably related to the glass composition, especially to a different extent of cross-linking of glass structure. The ion implantation process caused the different range of structure damage in glass (so called de-polymerization of the glass [31]) according to the glass composition and structure. Therefore, the subsequent annealing process results in different speed in the recovery of the glass matrix. Consequently gold nano-particles observed in glasses after the post-implantation annealing by TEM exhibit different size, shape and distribution.

The metal nano-particles absorb part of the UV–VIS spectra, which results in the coloration of the glass. The absorption of these glasses in the UV–VIS region is given by a characteristic surface plasmon resonance frequency of the metal nano-particles. The characteristic wavelength of the surface plasmon resonance of gold is centered around 535 nm [6], i.e. at wavelength observed also in our glasses. The results showed that the shape of the absorption band, its intensity and position in the spectrum are affected by the size, shape and distribution of nano-particles in the glass. The thinner layers (in which metal nano-particles are distributed in the glass) and the larger particle size both result in a better-defined absorption band. Decreasing the size of the gold nano-particles in the glass and extending the layer in which nano-particles are present result in shifting the absorption band toward shorter wavelengths.

The enhancement of the nonlinear response of the glass observed after implantation (in the case of BK7) and after annealing is caused due to the presence of gold nano-particles in glass. This is because of the phenomenon referred to as surface plasmon resonance: The electron gas in the nanoscale particles is forced to resonate by the oscillating electromagnetic field of the laser radiation. This results in an enhancement of the local electric field, and thus an increase in the optical nonlinear response of the metal nano-particles implanted in the glasses. This causes an increase of several orders of magnitude in optical nonlinear response of metal nano-particles compared to that of the bulk solid one.

From our data in Tables 2 and 3, it becomes evident that the size of the nano-particles is the most relevant factor for the TPA coefficient. Measurements of the linear absorption spectra also show that the characteristic surface plasmon resonance feature is maximal for the largest clusters [33–37].

Table 3
TPA coefficients of nano-composite glasses prepared by ion implantation in different silicate glasses under identical conditions.

Glass substrate	Silica glass	Glass B	GIL 49	BK 7
TPA coefficient (cm/GW)	2.46	5.21	7.75	16.25

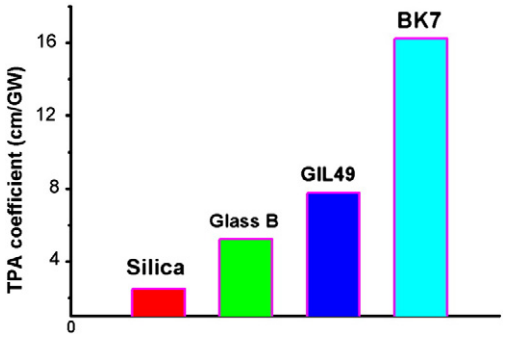

Fig. 5. TPA coefficients of nano-composite glasses prepared by ion implantation in different silicate glasses under identical conditions.

But also the shape and the layer thickness can have a substantial influence. Our results indicate that non-spherical nano-particles in glass BK7 show higher TPA coefficient than spherical ones in glass GIL49 and glass B. If the surface of a metal nano-particle is rough, the surface plasmons (SP) are strongly scattered leading to the accumulation of the electromagnetic field density [27]. This causes an enhancement of the local electric field and thus an increase in polarization. This is an indication of a susceptibility enhancement and a strong nonlinear response of the nano-composite material.

Moreover, our results showed that the composition and structure of the used glass have significant impact on the resulting nonlinear optical properties.

One should notice that the metal nonlinear response is indeed further amplified by the SPR phenomenon, which depends significantly on the difference of the dielectric constant of the nano-particles and the host medium. Therefore, the metal alone cannot explain by itself the highly nonlinear response of the nano-composite media. This indicates that the substrate plays an important role in two aspects: First, it affects the size, shape and distribution of the metal nano-particles formed in the composite material (which are responsible for the strength of nonlinear response of metal nano-particles) and secondly, as mentioned above, the dielectric contrast between the particles and the substrate is responsible for amplification of the local electric field which thus determines the strength of the nonlinear optical response of the metal nano-particles. Why BK7 develops the largest gold nano-particles and shows the highest TPA coefficient is still unclear and will be the subject of further investigation.

5. Conclusion

It was shown that the nucleation of gold nano-particles and their parameters (such as size, shape and distribution in glass matrix) depend on the glass composition and structure. It is due to the different extent of de-polymerization of the glass during the implantation and therefore the different conditions for the nucleation of the gold nano-particles.

We could establish that the increase of the TPA coefficient is mainly caused by increasing the size of gold nano-particles presented in the glass. The TPA coefficient ranges from 2.5 to 16.3 cm/GW depending on the glass composition and its structure, although we kept the conditions of the preparation of the nano-composite glass identical. The highest value of TPA coefficient was found for glass BK7 under these conditions: Au^+ implantation, beam energy of 1701 keV, ion fluence of 1×10^{16} ion cm^{-2}, post-implantation annealing in air at 600 °C for 5 h.

Acknowledgments

Some of us acknowledge the financial support by the Agency of the Czech Republic, grants LC06041, MSMT 6046137302 and MSM No. 21/2010 SPIRIT020.

References

[1] P.C.S. Kasap, Springer Handbook of Electronic and Photonic Materials, Springer, New York, 2006.
[2] N.N.H. Bach, The Properties of Optical Glass, Springer-Verlag, Berlin, 1998.
[3] R.L. Sutherland, Handbook of Nonlinear Optics, Marcel Dekker, New York, 2003.
[4] P. Chakraborty, Journal of Materials Science 33 (1998) 2235.
[5] R.W. Boyd, Nonlinear optics, Academic, San Diego, 2003.
[6] F. Gonella, P. Mazzoldi, Handbook of Nanostructured Materials and Nanotechnology, 4, Academic, San Diego, 2000.
[7] B. Palpant, Non-linear optical properties of matter, 1, Springer, 2006.
[8] W. Rechberger, A. Hohenau, A. Leitner, J.R. Krenn, B. Lamprecht, F.R. Aussenegg, Optics Communications 220 (2003) 137.
[9] A.I. Ryasnyanskiy, B. Palpant, S. Debrus, U. Pal, A.L. Stepanov, Optics Communications 273 (2007) 538.
[10] A. Lesuffleur, P. Gogol, P. Beauvillain, B. Guizal, D. Van Labeke, P. Georges, Journal of Applied Physics 104 (12) (2008) Art. No.: 124310.
[11] F.Z. Henari, A.A. Dakhel, Journal of Applied Physics 104 (3) (2008) Art. No.: 033110.
[12] W. Wang, Y. Wang, Z. Dai, Y. Sun, Applied Surface Science 253 (2007) 4673.
[13] A.I. Ryasnyanskiy, B. Palpant, S. Debrus, U. Pal, A. Stepanov, Journal of Luminescence 127 (2007) 181.
[14] N. Venkatram, R. Sai Santosh Kumar, D. Narayana Rao, S.K. Medda, S. De, G. De, Journal of Nanoscience and Nanotechnology 6 (2006) 1990.
[15] J.T. Seo, S.M. Ma, Q. Yang, R. Battle, L. Creekmore, B. Tabibi, W.J. Kim, J.H. Heo, W.S. Yun, D.H. Ha, S.S. Jung, E. Bryant, C. Payne, W. Yu, V. Colvin, Proceedings of the IEEE 1 (2006) 258.
[16] A.I. Ryasnyanskiy, B. Palpant, S. Debrus, U. Pal, A.L. Stepanov, Physics of the Solid State 51 (2009) 55.
[17] S. Sreeja, S. Mayadevi, S.R. Suresh, P.G.L. Frobel, N. Smijesh, R. Philip, C.I. Muneera, PRO 1391 (2011) 618.
[18] G. Vinitha, A. Ramalingam, Proceedings of World Academy of Science, Engineering and Technology, 64, 2010.
[19] H. Inouye, K. Tanaka, I. Tanahashi, T. Hattori, H. Nakatsuka, Japanese Journal of Applied Physics, Part 1: Regular Papers and Short Notes and Review Papers 39 (2000).
[20] E. Shahriari, W. Mahmood Mat Yunus, Digest Journal of Nanomaterials and Biostructures 5 (2010) 939.
[21] Y.H. Wang, F. Ren, Q.Q. Wang, D.J. Chen, D.J. Fu, C.Z. Jiang, Physics Letters, Section A: General, Atomic and Solid State Physics 357 (2006) 364.
[22] E. Cattaruzza, G. Battaglin, P. Calvelli, F. Gonella, G. Mattei, C. Maurizio, P. Mazzoldi, S. Padovani, R. Polloni, C. Sada, B.F. Scremin, F. D'Acapito, Composites Science and Technology 63 (2003) 1203.
[23] J. Olivares, J. Requejo-Isidro, R. Del Coso, R. De Nalda, J. Solis, C.N. Afonso, A.L. Stepanov, D. Hole, P.D. Townsend, A. Naudon, Journal of Applied Physics 90 (2001) 1064.
[24] C. Xu, W.W. Webb, Journal of the Optical Society of America B: Optical Physics 13 (1996) 481.
[25] J.D. Bhawalkar, G.S. He, P.N. Prasad, Reports on Progress in Physics 59 (1996) 1041.
[26] Q. Yang, J. Seo, S. Creekmore, G. Tan, H. Brown, S.M. Ma, L. Creekmore, A. Jackson, T. Skyles, B. Tabibi, H. Wang, S. Jung, M. Namkung, Journal of Physics Conference Series 38 (2006) 144.
[27] P. Wang, Y. Lu, L. Tang, J. Zhang, H. Ming, J. Xie, F.H. Ho, H.H. Chang, H.Y. Lin, D.P. Tsai, Optics Communications 229 (2004) 425.
[28] R.A. Ganeev, A.I. Ryasnyansky, A.L. Stepanov, C. Marques, R.C. Da Silva, E. Alves, Optics Communications 253 (2005) 205.
[29] M. Sheik-Bahae, A.A. Said, T.-H. Wei, D.J. Hagan, E.W. Van Stryland, IEEE Journal of Quantum Electronics 26 (1990) 760.
[30] P. Malinský, A. Macková, J. Bočan, B. Švecová, P. Nekvindová, Nuclear Instruments and Methods in Physics Research Section B: Beam Interactions with Materials and Atoms 267 (2009) 1575.
[31] B. Svecova, P. Nekvindova, A. MacKova, P. Malinsky, A. Kolitsch, V. Machovic, S. Stara, M. Mika, J. Spirkova, Journal of Non-Crystalline Solids 356 (2010) 2468.
[32] A. Ajami, W. Husinsky, R. Liska, N. Pucher, Journal of the Optical Society of America B: Optical Physics 27 (2010) 2290.
[33] Y.H. Wang, Y.M. Wang, J.D. Lu, L.L. Ji, R.G. Zang, R.W. Wang, Optics Communications 283 (2010) 486.
[34] S. Nah, L. Li, J.T. Fourkas, Journal of Physical Chemistry A 113 (2009) 4416.
[35] R. Sreeja, R. Reshmi, M. George, M.K. Jayaraj, Proceedings of SPIE 7155 (2008) Art. No.: 715521.
[36] X. Liu, Y. Tomita, K. Yasui, K. Kojima, K. Chikama, Proceedings of SPIE 7722 (2010) Art. No.: 77222A.
[37] J. Shin, K. Jang, K.S. Lim, I.B. Sohn, Y.C. Noh, J. Lee, Applied Physics A: Materials Science and Processing 93 (2008) 923.